

Non-Hermiticity in a kicked model: Decoherence and the semiclassical limit

Indubala I. Satija*

Department of Physics, George Mason University, Fairfax, Virginia 22030

Arjendu K. Pattanayak†

Department of Physics and Astronomy, Carleton College, Northfield, Minnesota 55057

(Received 15 January 2002; published 3 April 2002)

We study the effects of non-Hermitian perturbations on a quantum kicked model exhibiting a localization transition. Using an exact renormalization scheme, we show that the critical line separating the extended and localized phases approaches its semiclassical limit as the imaginary part of the kicking parameter is steadily increased. Further, the metastability of the quantum states appears to be directly correlated with the deviation between the semiclassical and quantum results. This direct evidence of quantum-classical correspondence suggests that decoherence may be usefully modeled by non-Hermitian perturbations.

DOI: 10.1103/PhysRevE.65.045205

PACS number(s): 05.45.-a, 74.60.Ge, 05.30.Jp, 42.50.Lc

Decoherence, namely, the loss of quantum coherence through perturbations from environmental degrees of freedom is one of the most exciting and active area of research at the forefront of physics. In addition to its importance at technological fronts such as quantum computing [1], the subject is crucial to the field of quantum chaos. It is argued that decoherence is essential in establishing the correspondence principle for quantum systems with classically chaotic limits [2]. The subject has created theoretical and experimental challenges in modeling and controlling the interaction of quantum systems with the environment.

There are recent suggestions that decoherence and dissipation may be modeled as non-Hermitian perturbations [3]. At the same time, there has been a considerable amount of interest in delocalization effects in non-Hermitian systems, although these have not considered the connection to decoherence at all. These studies were triggered by the result [4] that a complex vector potential delocalizes the wave functions that are otherwise localized in a random potential. This is reminiscent of the delocalization due to decoherence of dynamical localization in quantum systems with classically chaotic dynamics [5]. In this paper, we argue that effects of non-Hermiticity may be understood as a special case of the general effect of quantum properties being destroyed by decoherence. Among other interesting questions, this opens up the issue of characterizing the transition from quantum to classical properties as a function of the strength of the complex perturbation.

Earlier studies relating non-Hermitian perturbations and delocalization were confined to the complex vector potential. The non-Hermitian vector potential was argued to be intrinsically different from non-Hermitian scalar potentials [6] in that the imaginary vector potential singles out a direction in space, breaking the symmetry between the left- and the right-moving particles, while the imaginary scalar potential can be understood as singling out a direction in time. However, our results indicate that transport characteristics are *in general*

affected by non-Hermiticity *irrespective* of where the non-Hermitian terms appear. This line of reasoning emerged from a recent study of non-Hermitian lattice models exhibiting a localization-delocalization transition [7]. There, the non-Hermitian scalar and vector potentials correspond to the non-Hermitian diagonal and off-diagonal perturbations that are related by a Fourier transformation. That is, the effects on spatial localization due to the complex vector perturbation correspond to the effects on momentum space localization due to the scalar term. In particular, it was found that for a complex vector potential, the extended phase is accompanied by complex eigenenergies (as found earlier [4]) while for the complex scalar potential the same was true for the localized states. Thus, the main issue is the non-Hermiticity itself rather than its source in the vector or the scalar potential. This perspective specifically interprets non-Hermitian terms via their effects as decohering perturbations. In the following, we study a nonautonomous system, with non-Hermitian kicking, exhibiting a localization-delocalization transition. Using a renormalization group (RG) technique, we study the effects of non-Hermiticity on this transition. We show explicitly that as the non-Hermitian perturbation is increased, the system's localization-delocalization phase diagram monotonically approaches the semiclassically determined diagram.

Periodically kicked Hamiltonian systems such as

$$H = T(p) + V(x) \sum \delta(t-n), \quad (1)$$

with sinusoidally periodic $V(x)$ and $T(p) = p^2/2$ (kicked rotor) or $T(p) = L \cos(p)$ (kicked Harper), are an important class of theoretical and experimental systems for studying the quantum dynamics of classically nonintegrable systems [8]. Despite extensive study for almost two decades, questions of classical-quantum correspondence and dynamical localization in these systems remain open. When the quasienergy states of the system are projected on the angular momentum basis, these models map onto lattice models [9]. However, in contrast to the lattice models for autonomous systems, kicked systems yield long-range interactions and hence are more difficult to study. A special class of kicked

*URL: <http://physics.gmu.edu/~isatija>

†URL: <http://physics.carleton.edu/Faculty/Arjendu>

models with $V(x) = 2\hbar \arctan[\bar{K} \cos(x)]$ are useful [9,10] as they can be represented by a nearest-neighbor (NN) tight-binding model (tbm) of the form

$$\psi_{m+1} + \psi_{m-1} + \frac{2}{\bar{K}} \tan \left[\frac{T(\hbar m)}{2\hbar} - \frac{\omega}{2} \right] \psi_m = 0, \quad (2)$$

where ω is the quasienergy. Here the lattice index m represents the angular momentum quantum number in the absence of the kicking term.

With $T(p) = p^2/2$, this model resembles a lattice model with a pseudorandom potential exhibiting localization with the localization length equal to that of the Lloyd model [9,10]. We study the model with $T(p) = L \cos(p)$, which exhibits both extended and localized phases [13] for irrational $\hbar/2\pi$. The system also describes the NN truncation of the kicked Harper model, and for small \bar{K} and $\bar{L} \equiv L/2\hbar$, it reduces to the Harper equation [11] with $E = \omega$. This model is thus a good testing ground for investigating the effects of non-Hermitian perturbations on the transport characteristics of nonautonomous systems.

Although this model has no nontrivial classical limit, a nontrivial semiclassical limit does exist. The lattice representation of the model can be written as a quantum Hamiltonian [12–14] $\mathcal{H} = \bar{K} \cos(P) + \tan[\bar{L} \cos(X) - \omega/2]$ restricted to the Hilbert subspace defined by eigenvalue $E = 0$ where $X = \hbar m$ and $[X, P] = i\hbar$. This Hamiltonian, interpreted classically, has orbits in phase space, which may carry a signature of the localization-delocalization transition for the original lattice model. For the Harper equation, which describes an autonomous system, unbounded phase-space trajectories for $K \neq L$ are found to correspond to extended or localized states while a bounded orbit at $K = L$ describes the localization-delocalization boundary. Here the semiclassical prediction for the critical point is *exact*. For the kicked system discussed above, it is easy to show that the semiclassical Hamiltonian has bounded orbits provided $\bar{K} = \tan(\bar{L})$, independent of ω . This is, therefore, the semiclassical condition for the critical line separating the extended and localized states for the model in Eq. (2). We show below that this semiclassical critical line is a reasonable approximation to the “exact” quantum critical line, and for complex kicking, the exact critical line tends toward this semiclassical line.

The quantum phase diagram in $\bar{K} - \bar{L}$ space is studied using a RG approach for a fixed quasienergy. We use dimer decimation [15,16] that has conceptual and intuitive advantages over other RG schemes [17,18]. The key idea underlying the renormalization scheme is the *simultaneous* decimation of the two central sites of the doubly infinite lattice $-\infty, \dots, -2, -1, 0, 1, 2, \dots, \infty$, in the tbm, after we have eliminated the central site $m = 0$. At the n th step where all sites with $|m| < n$ have been decimated, the tbm for $m = \pm n$ reads

$$\Phi_{n+1} + G^+(n)\Phi_{-n} - E^-(n)\Phi_n = 0, \quad (3)$$

$$\Phi_{-n-1} + G^-(n)\Phi_n - E^+(n)\Phi_{-n} = 0, \quad (4)$$

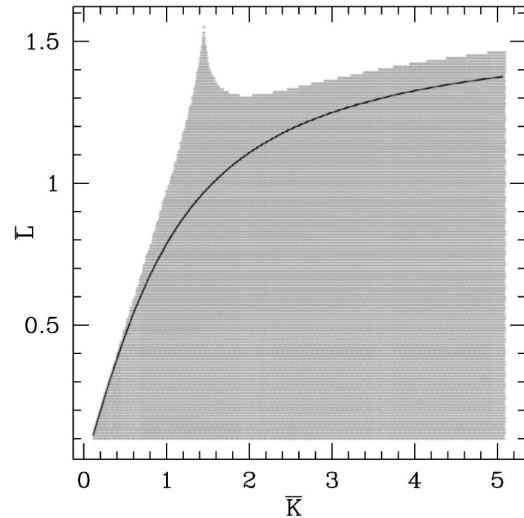


FIG. 1. Phase diagram for the kicked model with $\hbar/2\pi = (\sqrt{5} - 1)/2$ and $\omega = 0$. The shaded regime is the extended phase. The solid line is the semiclassical critical line.

where $G^x(n)$ and $E^x(n)$ ($x = \pm$), respectively, describe the renormalized coupling and the on-site potential term at the n th step of the renormalization. The initial values of the couplings are obtained from Eq. (2) after decimating the central site [15,16]. The $+$ ($-$) correspond to the right (left) parts of the lattice. In the model under investigation here, $G^- = G^+$ and $E^- = E^+$ due to $m \rightarrow -m$ symmetry. The renormalized parameters are given by the *exact* RG flow [15]

$$\mathbf{M}_{n+1} = \mathbf{f}_{n+1} + \mathbf{M}_n^{-1}, \quad (5)$$

where \mathbf{M} is a 2×2 matrix,

$$\mathbf{M} = \begin{pmatrix} E^- & G^- \\ G^+ & E^+ \end{pmatrix}, \quad (6)$$

and \mathbf{f} is a diagonal matrix, with elements E^{-1} and E^+ . Asymptotically, the renormalized lattice can be viewed as a dimer where the transport characteristics are determined by the quantum interference between the two sites of the dimer. Interestingly, the extended phase resembles a rigid dimer while the localized phase is asymptotically a broken dimer. Therefore, the transport properties are described by the effective coupling of the renormalized dimer, which is the ratio between the offdiagonal and the diagonal part of the renormalized tbm $R(n) = GG^\dagger/EE^\dagger$. The scaling exponent $\beta = \lim_{n \rightarrow \infty} \ln R(n)/\ln n$ effectively quantifies the transport properties, since extended states are described by (typically monotonic) convergence of $\beta(n) \rightarrow 0$. For exponential localization, $\beta(n) \rightarrow -\infty$. In contrast, the critical states are characterized by negative β and nonconvergent, oscillatory behavior.

Figure 1 shows the results, at almost machine precision, of this method applied to Eq. (2) for $\omega = 0$. The important feature to note is that as the kicking parameter increases, the diagram has a narrow reentrant phase (a peak) and a plateau. Interestingly, with the exception of the region near this peak,

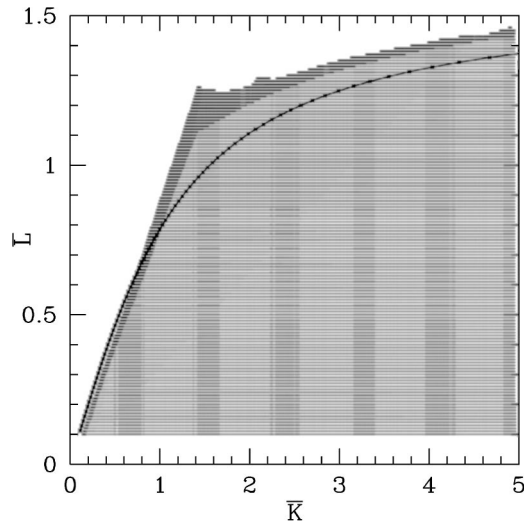


FIG. 2. Transport properties of a quantum wave packet. Using a plane wave initial condition, we compute $\langle p^2 \rangle$ after 1000 kicks. The lightly shaded regime shows the parameter space where $\langle p^2 \rangle$ is greater than 10^4 . The darker regime indicates that $\langle p^2 \rangle$ is between 10^3 – 10^4 . The narrowness of this regime confirms that the computation is converging accurately to the localization boundary.

the phase diagram is more or less consistent with the semiclassical prediction. Further, Fig. 2 shows the transport characteristics for wave packets in this system, and this global phase diagram closely resembles Fig. 1, which is for a pure quantum state. This is important, since RG tools to compute the phase diagram for $\omega=0$ require a small fraction of the computational time for computing the wave packet transport characteristics.

In Fig. 3, we show the effects of a complex perturbation, $\bar{K} \rightarrow \bar{K}_r + i\bar{K}_i$, on the phase diagram. The focus is on the

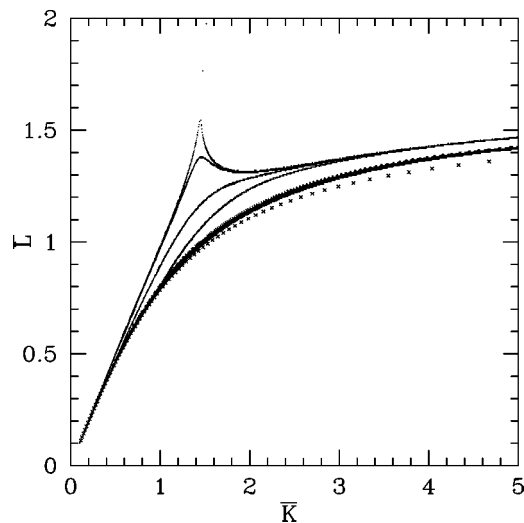


FIG. 3. The effects of complex perturbation on the critical line. The parameter \bar{K} is the absolute value of the complex kicking. The lines from top to bottom correspond to $\bar{K}_i=0, \bar{K}_i=0.1, \bar{K}_i=0.5, \bar{K}_i=1$, and finally with $\bar{K}_r=0$, respectively. The crosses show the semiclassical critical line.

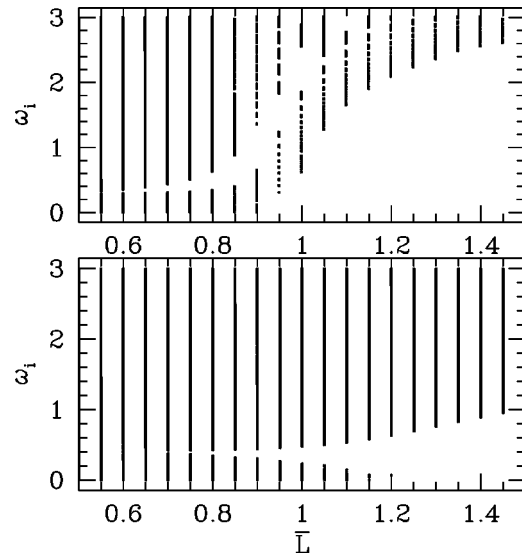


FIG. 4. The pure imaginary eigenvalues for $\bar{K}_r=0$ as the localization transition is approached, for $\bar{K}_i=1.5$ (top) and $\bar{K}_i=2.5$ (bottom). The figure shows only the extended states with $|\omega_i| < 3$; the spectrum is symmetric about $\omega_i=0$. A comparison between the top and the bottom figures shows that the peak part of the phase diagram is associated with shorter lifetimes and hence is more unstable.

changes in the critical line as \bar{K}_i is increased. What is interesting is the manner in which the transition curve moves towards the semiclassical critical line as the non-Hermiticity of the perturbation is increased. The transition appears to happen in distinct stages: (a) the peak diminishes and then disappears, (b) the curve gets closer in shape to the semiclassical line while still maintaining a difference, and finally, (c) when the real part of \bar{K} is switched off, the curve is almost exactly on top of the semiclassical line. Also, note that the effects of non-Hermiticity are consistent with the earlier work [4], since the non-Hermitian perturbation shifts the critical line in parameter space so as to increase the measure of parameter space corresponding to dynamical localization (for p or m in momentum space), and hence enhance the parameter space corresponding to delocalization in real space.

The RG approach was also used to study the effects of non-Hermiticity on the quasienergy spectrum [16]. It turns out that all quasienergies are in general complex [19]. Figure 4 shows the part of the spectrum with zero real part, i.e., the pure imaginary part of the eigenvalues. Analogous to the Bloch states (of a Hermitian model), the pure imaginary eigenvalues exhibit a *band structure*. It should be noted that we show only the *extended* states—these are easy to compute using the RG analysis [16]. As a result of the non-Hermiticity, the $\omega=0$ state has continuum families of lifetimes. Looking at this data, as we approach the localization-delocalization boundary, this band splits into subbands with the notable localization of the $\omega_i=0$ band at the onset of localization as confirmed by further simulations. The fact that the localization threshold is signaled by the $\omega_i=0$ band degenerating to a point, whence the state is localized with

both the real and imaginary part of the spectrum being point-like, is valid for other values of parameter as well.

An intriguing feature of this pure imaginary part of the spectrum is the presence of relatively large values of ω_i in the parameter regime for the *peak* of the phase diagram in Fig. 1. The results shown in Fig. 4 suggest that this region, where we also have extended states, is more unstable than the rest of the delocalized phase. This part of the parameter space corresponds to a greater deviation between the quantum and the semiclassical behaviors. As such, this implies that the $\omega=0$ quantum state is associated with relatively short lifetimes (is more unstable) when the system is in that part of parameter space that is *not* described semiclassically. This is consistent with the prediction from the decoherence literature, and the statement that the part of the phase diagram which is not described by the semiclassical theory is most sensitive to the non-Hermitian perturbation is arguably general.

Previous work has indicated that complex Hamiltonians may be associated with decoherence effects [3,20,21]. The

signature of decoherence is that the quantum system behaves increasingly classically as the decoherence parameter is increased, independent of the value of \hbar . Decoherence is in fact argued to be necessary for quantum-classical correspondence in chaotic systems [2,22]. Our results are consistent with this, showing that results from decoherence may be used to understand complex Hamiltonians, and alternatively, that a complex Hamiltonian formulation may be used to model decoherence effects. This opens new possibilities in modeling the interaction between nonintegrable systems and the environment, providing a simpler alternative to solving master equations [23]. We hope that our study will stimulate further exploration of non-Hermitian systems, and particularly of those displaying chaos.

We thank Tomaz Prosen and Nausheen Shah for their assistance in certain aspects of the work. The research of I.I.S. was supported by a grant from the National Science Foundation (Grant No. DMR 0072813).

-
- [1] See, for example, M.A. Nielsen and I. L. Chuang, *Quantum Computation and Quantum Information* (Cambridge University Press, New York, 2000).
- [2] W.H. Zurek and J.P. Paz, *Physica D* **83**, 300 (1995).
- [3] D. Ferry and J.R. Barker, *Appl. Phys. Lett.* **74**, 582 (1999).
- [4] N. Hatano and D.R. Nelson, *Phys. Rev. Lett.* **77**, 570 (1996); *Phys. Rev. B* **56**, 8651 (1997).
- [5] H. Ammann *et al.*, *Phys. Rev. Lett.* **80**, 4111 (1998); B.G. Klappauf *et al.*, *ibid.* **81**, 1203 (1998).
- [6] P.W. Brouwer, P.G. Silvestrov, and C.W.J. Beenakker, *Phys. Rev. B* **56**, R4333 (1997).
- [7] A. Jazaeri and I.I. Satija, *Phys. Rev. E* **63**, 036222 (2001).
- [8] *Quantum Chaos: Between Order and Disorder: A Selection of Papers*, edited by G. Casati and B. V. Chirikov (Cambridge University Press, New York, 1995).
- [9] See, D.R. Grempel, S. Fishman, and R.E. Prange, *Phys. Rev. A* **29**, 1639 (1984).
- [10] I.I. Satija, B. Sundaram, and J.A. Ketoja, *Phys. Rev. E* **60**, 453 (1999).
- [11] P.G. Harper, *Proc. Phys. Soc., London, Sect. A* **68**, 874 (1955).
- [12] M. Wilkinson, *Proc. R. Soc. London, Ser. A* **391**, 305 (1984).
- [13] For Hermitian kicking, this model was investigated by I. I. Satija and B. Sundaram (unpublished).
- [14] I.I. Satija and B. Sundaram, *Phys. Rev. Lett.* **84**, 4581 (2000).
- [15] I. Gomez and I.I. Satija, *Phys. Lett. A* **268**, 128 (2000).
- [16] T. Prosen, I.I. Satija, and N. Shah, *Phys. Rev. Lett.* **87**, 066601 (2001).
- [17] S. Ostlund and R. Pandit, *Phys. Rev. B* **29**, 1394 (1984).
- [18] J.A. Ketoja, *Phys. Rev. Lett.* **69**, 2180 (1992).
- [19] The $\omega=0$ eigenvalue continues to exist in real space also, which may be a consequence of some special symmetry of this state. See, for example, C.M. Bender and S. Boettcher, *Phys. Rev. Lett.*, **80**, 5243 (1998).
- [20] J. Wilkie, *J. Chem. Phys.* **115**, 10 335 (2001).
- [21] J. Audretsch and M. Mensky, *Phys. Rev. A* **56**, 44 (1997).
- [22] A.K. Pattanayak, *Phys. Rev. Lett.* **83**, 4526 (1999).
- [23] S. Habib *et al.*, *Phys. Rev. Lett.* **80**, 4361 (1998).